BUTTERWORTH HEINEMANN

Polymer Vol. 36 No. 17, pp. 3301–3312, 1995

0032-3861/95/$10.00+0.00

Glass–rubber constitutive model for amorphous polymers near the glass transition

C. P. Buckley* and D. C. Jones†
Department of Engineering Science, University of Oxford, Parks Road, Oxford OX1 3PJ, UK
(Received 20 September 1994; revised 22 December 1994)

The constitutive behaviour of amorphous polymers near the glass transition contains many features general to this class of materials. A new, physically based, three-dimensional constitutive model has been developed for simulating this wide range of features in models of polymer products and processes. In particular, the model displays glassy response at low temperatures and short time-scales, and rubber-like response at high temperatures and long time-scales, and is therefore an example of a glass–rubber constitutive model. Its basis is the assumed additivity of free energies of bond distortion and conformation perturbation. For the elastic bond distortion stress–strain law and flow model, and the conformational entropy function, the model employs linear elasticity, Eyring viscous flow and the Edwards–Vilgis entropy function, respectively. Glass structure and temperature dependence are introduced through the Vogel–Tammann–Fulcher and Arrhenius equations for viscosity, respectively. With parameters obtained for poly(ethylene terephthalate) in a companion paper, the model was solved numerically to simulate a variety of uniaxial strain sequences, and found to replicate well the characteristic patterns of behaviour of amorphous polymers in the temperature region of interest, over a wide range of experimental situations from small to large strains. The only major deficiency, resulting from the simplifying assumption of a single activation barrier height, is its being too localized in the time domain. At high temperatures and long times, applicability of the model is limited by the onset of conformational relaxation.

(Keywords: constitutive model; amorphous polymers; glass transition)

INTRODUCTION

There is considerable interest at present in three-dimensional constitutive modelling of materials. Computer-aided analysis tools are becoming widely used in design of products and processes, and to make accurate predictions they must be fed with accurate material models. But for polymers such models do not yet exist. These materials display a rich variety of non-linear phenomena in their constitutive behaviour, and the task of finding means of describing them mathematically poses a real challenge.

This paper shows, however, that the picture is not as complex as might be supposed. Progress is possible by exploiting two facts. First, with the availability of computational tools it is no longer necessary to hunt for a single elusive constitutive equation (stress/strain/time relation). Instead, a material may be represented by a set of simultaneous non-linear differential equations, solved numerically with a time-marching scheme to predict its response under the stress/strain/temperature history of interest. This offers hope of being able to simulate the many intricacies of polymer constitutive behaviour, that have so far defied description in terms of simpler models. Second, the last 30 years have seen intensive research on the physics of polymer deformation, and physical models have been developed that describe well several of the individual effects observed. The question that remains is how to combine these into a holistic description of polymer behaviour under conditions of engineering interest.

We consider here the deformation of uncrosslinked amorphous polymers near the glass transition. By this is meant the temperature range which for most polymers is bounded from below by the onset of microscopically visible non-uniform deformation zones, crazing or brittle fracture of unnotched specimens, and from above by the onset of permanent deformation due to escape of molecules from the topological constraint of others (a process referred to below by the term 'entanglement slippage'). It is the region where an amorphous polymer displays the characteristics of a homogeneously deforming ductile glass and/or those of a rubber. This is important in several major industrial processes, especially hot-drawing of fibres and films, thermoforming and blow-moulding of bottles. Of course, the temperature position and breadth of this region depend on molecular weight and chemical structure.

We show that a unifying framework for constitutive modelling of polymers under these conditions can be constructed, by combining a set of three different physical processes in a three-dimensionally self-consistent manner. Remarkably, it appears capable of capturing

* To whom correspondence should be addressed
† Present address: Fisons Instruments, 3 Tudor Road, Altrincham, Manchester WA14 5RZ, UK

a very wide range of observed features of constitutive response. Several aspects of the model have been employed already by the authors and others in specific contexts. But it has not been shown before that, when assembled together in an appropriate manner, they provide a unifying account of a large number of constitutive phenomena, some of them previously treated as unrelated.

Early attempts to model polymer deformation focused mostly on specific aspects of behaviour or underlying physical processes in isolation: linear viscoelasticity (in integral or differential form), non-linear viscoelasticity (also expressed in integral or differential forms), yield and flow (especially stress state and rate dependence), or rubber elasticity. Until recently, only a few authors had attempted unification, to encompass in one mathematical model more than one physical feature. It is widely recognized, however, that the physics of solid-state deformation of amorphous polymers involves both a flow process and the elastic deformation of an entangled molecular network, as has been amply demonstrated over many years, most notably by Ward and co-workers[1]. Haward and Thackray[2] combined a yield/flow model (based on the Eyring theory[3]) with rubber elasticity (the theory of James and Guth[4] was employed, leading to the well-known 'inverse Langevin' stress–strain relation), to give a unified mathematical description of yield, drawing and strain stiffening in thermoplastics. Such a model, combining features characteristic both of a glass and a rubber, might be termed a glass–rubber constitutive model. As proposed by Haward and Thackray, however, it was a one-dimensional model, for calculating the response in a uniaxial tensile test, and corresponded to a non-linear form of the Zener viscoelastic model (rubber-elastic spring in parallel with a series combination of linear elastic spring and Eyring dashpot). The potential of this kind of approach has been explored more fully by Boyce and co-workers[5–7]. They extended the model to three dimensions and replaced the Eyring flow model by the 'double-kink' model of molecular deformation in the glassy state, due to Argon[8]. The Boyce model has found considerable success in fitting stress–strain curves in the glassy state, has been employed within stress analyses to predict inhomogeneous deformation[6,9], and has been extended to prediction of the development of anisotropy in deformed polymer glasses[10,11]. The present authors and others have applied further three-dimensional variants of the Haward–Thackray approach to specific problems, varying the form of flow model and rubber stress–strain relation assumed[12–16]. But the important question, not yet addressed is: can such models accommodate the full range of features of polymer constitutive behaviour? It is an interesting fact that a large number of these seem to be inherent in polymers, and occur irrespective of chemical composition. Consequently, a constitutive model for polymers should be judged on whether it displays these features naturally, without need for empirical modification.

Consider the following well-documented facts of the deformation of uncrosslinked, amorphous polymers in the regime of interest.

1. At the smallest strains (less than $\sim 0.5\%$) the behaviour is described by the theory of linear viscoelasticity, with relaxation times dependent on temperature and structural (i.e. 'ageing') state.
2. Linear viscoelastic responses show time–temperature superposition to a good approximation, with relaxation times appearing to follow the Williams–Landel–Ferry (WLF) equation above the glass transition temperature T_g, but having a lower temperature coefficient below it.
3. Following a quench from above T_g to below, linear viscoelastic relaxation times increase with ageing time.
4. At larger strains (~ 0.5 to 5%) the behaviour is non-linear viscoelastic, exhibiting a variety of manifestations of non-linearity that appear to be general. Among these are: (a) strain softening; (b) greater stiffness in compression than in tension; (c) time-dependent stiffening with respect to additional strains, when superposed on an existing (constant) stress or strain.
5. In tension or compression tests, Poisson's ratio increases from ~ 0.3 to a limiting value of 0.5, with increasing strain, time or temperature.
6. With further increase in strain, there occurs an apparent 'yield' where strain increases at constant or even decreasing stress, this strain being apparently permanent on removal of stress. It is well known, however, that the strain is at least partially recoverable: a rise in temperature, under zero load, will cause the strain to decay rapidly.
7. When yield is observed in tests with various strain states, the stresses at yield usually obey (to a good approximation) a pressure-modified von Mises yield criterion.
8. If the test is repeated at various strain rates, with a particular strain state, the yield stresses are usually observed to be a linear function of log(strain rate) (the well-known Eyring plot).
9. If the test is repeated at various temperatures, the yield stress falls with increasing temperature, showing a higher temperature coefficient above T_g than below.
10. If the test is repeated at various structural states obtained by physical ageing below T_g following a quench, the yield stress increases with ageing time.
11. At high strains (of the order of unity) there is pronounced strain stiffening known to be associated with increasing molecular orientation, and other evidence suggests the polymer behaves as a rubbery molecular network.

This paper demonstrates that a glass–rubber constitutive model, suitably constructed, encompasses naturally the full range of phenomena listed above. For the purpose of illustration, we use a set of parameters obtained by fitting the model to experimental data for the hot-drawing of amorphous poly(ethylene terephthalate) (PET), as described in a companion paper[17].

THE CONSTITUTIVE MODEL

Structure of the model

We begin by deriving a new three-dimensional glass–rubber constitutive model, structured in such a manner as to expose more readily than previous models how it behaves right across the range of observed phenomena.

The model is physically based, combining in a three-dimensionally self-consistent manner several existing theories of different aspects of polymer deformation.

Consider an amorphous, isotropic polymer subject to an isothermal, irrotational deformation where a general point at position vector $\boldsymbol{X}$ moves to $\boldsymbol{x}$, as characterized by the stretch tensor

$$\boldsymbol{\Lambda} = \frac{\partial \boldsymbol{x}}{\partial \boldsymbol{X}} \tag{1}$$

whose eigenvalues are the principal stretches λ_i $(i = 1, 2, 3)$.

It is well known that a deformed amorphous polymer stores strain energy by two mechanisms: perturbation of interatomic potentials (inter- and intramolecular) that we refer to here as 'bond stretching'; and perturbation of configurational entropy through change of molecular conformations. We assume here that the contributions of these two phenomena to the free energy are additive. This can be expressed concisely in the statement that the free energy density function A is the sum of two parts, A^b and A^c, associated with bond stretching and conformational change, respectively. From the first and second laws of thermodynamics, nominal stresses at any instant can always be expressed as gradients of A with respect to a hypothetical, thermodynamically reversible, isothermal deformation. Principal values of the Cauchy (true) stress tensor $\boldsymbol{\Sigma}$ may thus be expressed as the sum of two parts:

$$\sigma_i = \sigma_i^b + \sigma_i^c \tag{2}$$

$$\sigma_i = \frac{1}{\det \boldsymbol{\Lambda}} \left(\frac{\partial A}{\partial \ln \lambda_i} \right)_{\text{rev}} = \frac{1}{\det \boldsymbol{\Lambda}} \left(\frac{\partial A^b}{\partial \ln \lambda_i} + \frac{\partial A^c}{\partial \ln \lambda_i} \right)_{\text{rev}} \tag{3}$$

The stress tensor $\boldsymbol{\Sigma}$ clearly has two parts, $\boldsymbol{\Sigma}^b$ and $\boldsymbol{\Sigma}^c$: a 'bond stretching stress' and a 'conformational stress' arising from the dependences on $\boldsymbol{\Lambda}$ of A^b and A^c, respectively. The change of molecular conformations is assumed here to occur reversibly in response to deformation, so the conformational stress can be obtained directly from

$$\sigma_i^c = \frac{1}{\det \boldsymbol{\Lambda}} \frac{\partial A^c}{\partial \ln \lambda_i} \tag{4}$$

On the other hand, bond stretching has an irreversible component. The glass transition region is understood to mark the onset of main-chain segmental motion which may be considered as the continual rupture and reformation of intermolecular bonds. Hence a portion of any deformation represents an irreversible flow of segments past their neighbours and does not contribute to A^b, acting as a viscous stretch $\boldsymbol{\Lambda}^v$. The reversible component of bond stretching corresponds to an elastic stretch $\boldsymbol{\Lambda}^e$, such that A^b (and hence $\boldsymbol{\Sigma}^b$) is a unique function of $\boldsymbol{\Lambda}^e$. The two components of stretch can be assumed to combine multiplicatively[18]

$$\boldsymbol{\Lambda} = \boldsymbol{\Lambda}^v \boldsymbol{\Lambda}^e \tag{5}$$

At the stresses reached under the conditions of interest here, $\boldsymbol{\Lambda}^e$ corresponds to small strains (of the order of 10^{-2} at most). In view of this and the polymer's assumed isotropy, the relation between $\boldsymbol{\Sigma}^b$ and $\boldsymbol{\Lambda}^e$ is that of isotropic linear elasticity. In terms of the mean and deviatoric components of stress

$$\sigma_m^b = \tfrac{1}{3}\text{tr}\boldsymbol{\Sigma}^b; \qquad \mathbf{S}^b = \boldsymbol{\Sigma}^b - \sigma_m^b \mathbf{I} \tag{6}$$

it may be written in component form as

$$\ln \lambda_i^e = \frac{\sigma_m^b - \sigma_{m0}^b}{3K^b} + \frac{s_i^b}{2G^b} \tag{7}$$

where K^b and G^b are the contributions to bulk and shear moduli arising from bond stretching, and σ_{m0}^b is the initial internal energy elastic stress present in rubbery polymers[19].

The flow process

For amorphous polymers at the glass transition, the magnitude of shear relaxation is known greatly to exceed volume relaxation (by a factor of 10^2 to 10^3)[20]. Consequently we approximate the flow described by $\boldsymbol{\Lambda}^v$ as occurring at constant volume, and to be that of an isotropic non-Newtonian viscous fluid

$$\mathbf{D}^v = \frac{\mathbf{S}^b}{\mu} \tag{8}$$

where $\mathbf{D}^v$ is the rate of deformation tensor

$$\mathbf{D}^v = \frac{\mathrm{d}\boldsymbol{\Lambda}^v}{\mathrm{d}t} \boldsymbol{\Lambda}^{v^{-1}} \tag{9}$$

and the generalized viscosity μ is some function of the invariants of $\boldsymbol{\Sigma}^b$, temperature and the structural state of the polymer.

The detailed molecular displacements involved in plastic deformation of amorphous polymers near T_g are not known. We invoke therefore a rather general description in terms of the theory of activated rate processes, following Eyring[3]. The activation event is taken to be a discrete viscous deformation of volume V of material obeying equation (8), and it follows that the work ΔW done by the stress system can be expressed in terms of the shear stress and increment of viscous shear strain, τ_{oct}^B and $\Delta\gamma_{oct}^v$, on the octahedral plane:

$$\Delta W = \frac{3V}{2} \Delta\gamma_{oct}^v \tau_{oct}^b \tag{10}$$

where

$$\tau_{oct}^b = \sqrt{\tfrac{1}{3}\text{tr}(\mathbf{S}^b)^2}$$

$$= \tfrac{1}{3}\sqrt{(\sigma_1^b - \sigma_2^b)^2 + (\sigma_2^b - \sigma_3^b)^2 + (\sigma_3^b - \sigma_1^b)^2} \tag{11}$$

and the shear rate is d_{oct}^v, given similarly in terms of principal deformation rates. Applying equation (8) to shear on the octahedral plane, for example, yields a relation between them

$$d_{oct}^v = \frac{\tau_{oct}^b}{\mu} \tag{12}$$

Eyring's theory provides a form for the function μ. Suppose the molar free enthalpy barrier for self-diffusion of backbone chain segments in the absence of shear stress is ΔG. Then Eyring analysis predicts the octahedral shear rate to be given by

$$d_{oct}^v = \kappa \frac{k_B T}{h} \exp\left(\frac{-\Delta G}{RT}\right) \sinh\left(\frac{V_s \tau_{oct}^b}{2RT}\right) \tag{13}$$

where κ is a constant relating rate of strain to the jump frequency, accounting for the interchain co-operation required, and V_s is known as the 'shear activation

volume' defined as

$$V_s = \frac{3V}{2}\Delta\gamma_{oct} \tag{14}$$

Evidence from the behaviour of glasses near T_g indicates that ΔG is the sum of two terms: a structure-independent term ΔG_0, in the absence of applied stress, and a structure-dependent term. The latter is the subject of considerable debate in the literature of organic and inorganic glasses – see, for example, the review by Scherer[21]. According to the Cohen–Turnbull free volume model[22], it derives from the limited probability of agglomeration of sufficient free space at the activation site. This probability is proportional to $\exp[-C/(T_f - T_\infty)]$, where C and T_∞ are material constants and T_f is the fictive temperature characterizing the structure of the glass (temperature at which the material would have the same viscosity in equilibrium). It can be incorporated into the activation entropy

$$\Delta S = \Delta S_0 - \frac{RC}{T_f - T_\infty} \tag{15}$$

In general there will be a further contribution to ΔG, arising from the lower molecular packing density in the transition state. Work is then done by the mean stress, in both forward and backward activation steps, modifying the enthalpic component of the free enthalpy barrier:

$$\Delta H = \Delta H_0 - V_p \Delta\sigma_m^b \tag{16}$$

where $\Delta\sigma_m^b = \sigma_m^b - \sigma_{m0}^b$, and V_p is a constant with units of volume. By analogy with V_s, it may be termed the 'pressure activation volume'.

Equations (12), (13), (15) and (16) may be combined, to express the viscosity function μ as follows

$$\mu = \mu_0 \left(\frac{V_s \tau_{oct}^b}{2RT}\right) \frac{\exp\left(\dfrac{-V_p \Delta\sigma_m^b}{RT}\right)}{\sinh\left(\dfrac{V_s \tau_{oct}^b}{2RT}\right)} \tag{17}$$

where μ_0 is the viscosity in the low stress (Newtonian) limit and in turn may be expressed in terms of T, T_f and its value μ_0^* at some reference state T^*, T_f^*:

$$\mu_0 = \mu_0^* \exp\left(\frac{C}{T_f - T_\infty} - \frac{C}{T_f^* - T_\infty} + \frac{\Delta H_0}{RT} - \frac{\Delta H_0}{RT^*}\right) \tag{18}$$

Inspection of equations (17) and (18) reveals that μ satisfies the requirements of equation (8): it depends on temperature T, structure through T_f, and stress $\boldsymbol{\Sigma}^b$ through only its invariants $\Delta\sigma_m^b$ and τ_{oct}^b. We note that equation (18) is simply the hybrid, i.e. free volume + Arrhenius, expression for viscosity proposed some years ago for liquids by Macedo and Litovitz[23].

Conformational free energy

The final step in building the model is to invoke a specific form for the conformational free energy function $A^c(\boldsymbol{\Lambda})$. This presents a problem, as there is no physical model yet available for the development of conformational entropy through the glass transition, as molecular mobility increases. All that is possible at present is to assume that molecular mobility is fully developed, and all molecular conformations are sampled within the time-scale of interest (clearly untenable at low strains and temperatures well below T_g, but justified post-yield and in the proximity of T_g and above). In this approximation, the statistical theory of rubber elasticity applies. The molecule can be represented as a chain of freely orienting segments, whose motion is constrained topologically along its length by 'entanglements' provided by other molecules. A convenient physical theory is that provided by Edwards and Vilgis[24] for crosslinked, entangled polymers. The present case of an uncrosslinked polymer may be considered as a limit of the Edwards–Vilgis theory, when the density of crosslinks vanishes compared with the density of entanglements.

In the theory, an entanglement is represented by a 'slip-link' which allows the molecule a finite degree of axial mobility, characterized by the dimensionless parameter η ($\eta = 0$ for a crosslink). Inextensibility of the entangled network is introduced by the further parameter $\alpha = l/a$, where l is the freely orienting segment length and a the distance between entanglements. If the portion of a chain between entanglements is assumed a random walk, containing say n segments, we have

$$a^2 = nl^2 \tag{19}$$

It is clear that the limiting stretch of the network will be

$$\lambda_{max} \approx nl/a = \sqrt{n} = \alpha^{-1} \tag{20}$$

The entropic free energy function derived by Edwards and Vilgis[24] has the following form in the limit of no crosslinks:

$$A^c = \frac{N_e k_B T}{2}\left(\frac{(1+\eta)(1-\alpha^2)}{\left(1-\alpha^2\sum\lambda_i^2\right)}\sum\frac{\lambda_i^2}{1+\eta\lambda_i^2} + \sum\ln(1+\eta\lambda_i^2) + \ln\left(1-\alpha^2\sum\lambda_i^2\right)\right) \tag{21}$$

(all the summations are over $i = 1$ to 3), where N_e is the number of entanglements per unit volume. Equation (21) reduces to the classical Gaussian limit when $\alpha = \eta = 0$.

BEHAVIOUR OF THE MODEL

The results given above may be combined to form a system of coupled non-linear equations, that together represent the three-dimensional constitutive behaviour of the polymer. For each principal direction there is a stress balance (equation (3)) which may be written

$$s_i^b + K^b \sum_{j=1}^{3} \epsilon_j + \sigma_{m0}^b + \sigma_i^c - \sigma_i = 0 \tag{22}$$

where ϵ_j are principal natural strains $\ln\lambda_j$; deviatoric stresses s_i^b obey

$$\frac{ds_i^b}{dt} + \frac{s_i^b}{\tau} = 2G^b \frac{de_i}{dt} \tag{23}$$

in which e_j are the corresponding deviatoric strains and the time constant $\tau = \mu/2G^b$; and conformational stresses σ_i^c are given by equation (4). Non-linearity enters through the dependence of μ on $\Delta\sigma_m^b$ and τ_{oct}^b, and the non-linear strain dependence of σ_i^c.

Table 1 Model parameters proposed for PET by Buckley *et al.*[17]

Unrelaxed shear modulus, G (MPa)	600
Bulk modulus, K (MPa)	1800
Viscosity μ_0 in equilibrium at 67°C (GPa s)	5852
Constant, C (K)	1002
Limiting temperature, T_∞ (°C)	33.3
Activation enthalpy, ΔH_0 (kJ mol^{-1})	123
Shear activation volume, V_s (m^3 mol^{-1})	7.23
Pressure activation volume, V_p (m^3 mol^{-1})	1.35
Entanglement density, N_e (m^{-3})	1.67×10^{-26}
Slip-link mobility factor, η	0
Inextensibility factor, α	0.180

In the companion paper[17], a scheme is presented for obtaining the various material parameters from experimental data, and it is applied to data for amorphous poly(ethylene terephthalate) (PET). Amorphous PET provides a particularly useful illustration, because it is one of the most widely studied polymers across the full range of strains and temperatures. Moreover, it is known to crystallize at large strains (beyond 100–200%). Although this might be expected to lead to deviations from a model for amorphous polymers, in practice strain stiffening and optical properties during large deformations of PET show good consistency with the behaviour of a rubber-like network[1]. Presumably this is because the onset of crystallization locks the molecular network, deferring the onset of entanglement slippage. *Table 1* summarizes the values obtained for PET. They are employed in the following paragraphs to demonstrate the behaviour of the model in particular circumstances.

Some insight can be gained by analytical treatment of limiting cases. More generally, a numerical solution is needed. For the purpose of the present study a computer program was written for numerical analysis of uniaxial stretching under isothermal and isostructural conditions, employing finite-difference approximations of the time differentials and the Newton–Raphson method of solving the resulting non-linear simultaneous equations. A variable time-step size was used, to ensure stability and to impose a ceiling on numerical error in the finite-difference approximations.

The unstressed state

The reader will note that rubber-like conformational entropy is an integral feature of the model, but there is no externally imposed condition of incompressibility. Constraint on volume change enters naturally through the elasticity of bond stretching. It is well known that, according to the classical statistical theory of rubber elasticity, maximization of conformational entropy, acting alone, would cause a polymer network to collapse upon itself. In reality collapse is prevented by the excluded volumes of atoms, in other words by short-range bond stretching interactions. It is thus clear, even in the absence of a net external stress, that there is a hydrostatic conformational tension σ_{m0}^c which is balanced by a hydrostatic bond stretching compression σ_{m0}^b. These stresses occur naturally in the present model. By differentiation of the Edwards–Vilgis free energy function, equation (21), it may be shown that the initial stresses are

$$\sigma_{m0}^c = -\sigma_{m0}^b = N_e k_B T \left(\frac{1+\alpha^2}{1-3\alpha^2} + \frac{\eta}{1+\eta} \right) \qquad (24)$$

They are not insignificant in comparison with stresses involved in hot-drawing, for example. For PET at 100°C, their magnitude is ~1 MPa.

Linear viscoelasticity

In the linear limit of vanishingly small applied stresses, it is clear from equation (23) that the deviatoric bond stretching stress response is linear viscoelastic, with single relaxation time $\tau_0 = \mu_0/2G^b$. The bond stretching hydrostatic response has been assumed linear elastic with bulk modulus K^b: see equation (7). Similarly, in the linear limit the conformation stress response is linear elastic, giving contributions G^c and K^c to the shear and bulk moduli, respectively. Their values may be found by double differentiation of A^c for the cases of pure shear and pure dilation, respectively. Adding bond stretching and conformational components, the total deviatoric stress may then be seen to obey the differential equation of a general, single relaxation time, linear viscoelastic solid, with τ_0 the relaxation time, $\tau_0(1 + G^b/G^c)$ the retardation time, and G^c and $G^b + G^c$ the relaxed and unrelaxed shear moduli, respectively:

$$\frac{ds_i}{dt} + \frac{s_i}{\tau_0} = 2(G^b + G^c)\frac{de_i}{dt} + 2G^c\frac{e_i}{\tau_0} \qquad (25)$$

The total mean stress displays linear elasticity with bulk modulus $K^b + K^c$

$$\sigma_m = (K^b + K^c)\sum_{j=1}^{3} \epsilon_j \qquad (26)$$

although the contribution of K^c (which may be negative) is only $\sim 10^5$ Pa and therefore negligible compared with that of K^b, which is $\sim 10^9$ Pa.

To demonstrate linear viscoelastic response, uniaxial tensile stress relaxation tests were simulated with the numerical model. A 10^{-2} s ramp in tensile strain was applied, to produce a strain of 10^{-5} which was then held constant. Under these conditions the simulated material behaviour was essentially linear viscoelastic, with μ departing from μ_0 by less than 0.15%. Temperatures were chosen close to and above the glass transition where structural equilibrium obtains ($T_f = T$). Axial stress was divided by the axial strain to express it as the tensile stress relaxation modulus. The calculated tensile stress relaxation is shown in *Figure 1* and, as expected from equation (25), exhibits the well-known temperature-shifted stress relaxation observed in amorphous polymers in structural equilibrium near T_g.

The lateral contraction strain calculated in the same simulations is expressed as Poisson's ratio ν in *Figure 2*. It shows a steady rise from 0.35, characteristic of a polymer glass, to the usual rubbery value of 0.5, as expected from the fact that the shear modulus exhibits relaxation but the hydrostatic response is assumed elastic (equation (26)). Experimental reports of the time dependence of ν are sparse, but measurements of Poisson's ratio during stress relaxation of a (cross-linked) epoxy resin at various temperatures were made by Theocaris and Hadjijoseph[25]; the same pattern of temperature-shifted transition from a value characteristic of a glass to that of a rubber, as seen in *Figure 2*, was revealed.

Similar simulations were carried out for stress relaxation in the non-equilibrium state below T_g. For a

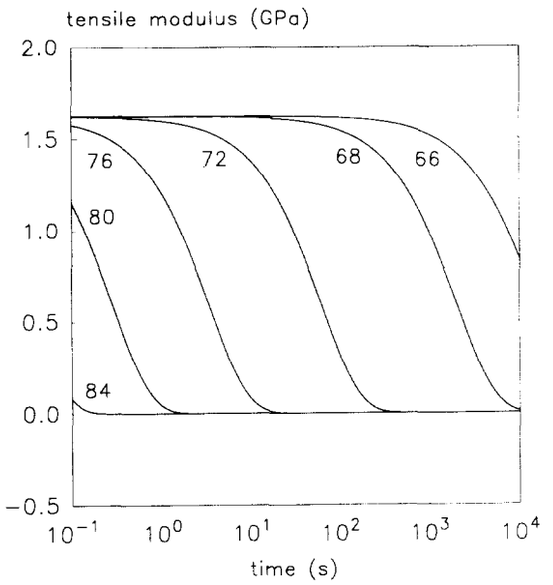

Figure 1 Simulations of tensile stress relaxation of PET in the linear viscoelastic region, for samples in equilibrium at the temperatures (°C) shown. A strain of 1×10^{-5} was applied to the model in a 10^{-2} s ramp. and then held constant. Calculated tensile stress is expressed as stress relaxation modulus

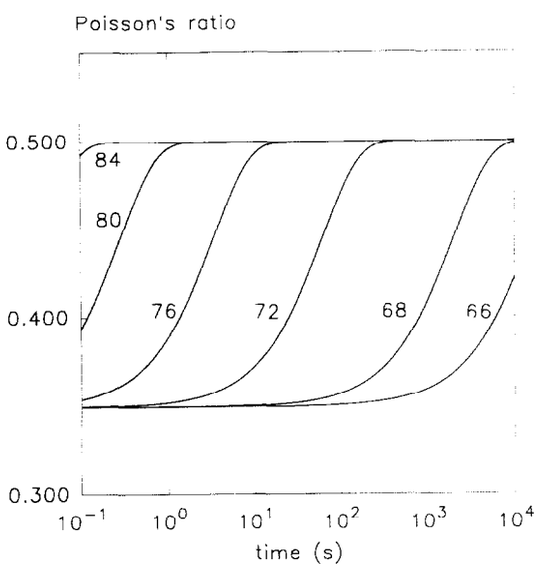

Figure 2 Lateral contraction as calculated in the same simulations as *Figure 1*, expressed as Poisson's ratio

constant temperature of 50°C, stress relaxation was simulated for several values of fictive temperature T_f, decreasing the fictive temperature corresponding to physical ageing. Results shown in *Figure 3* reveal the well-known shift of time-scale with ageing state that has been widely observed experimentally during physical ageing of amorphous polymers[26]. The major discrepancy between these results and experiment, of course, is the well-known breadth of the glass transition process in the time (and frequency) domain as observed experimentally, greatly exceeding that shown by the single relaxation time representation used here.

Since the model has only a single relaxation time, and

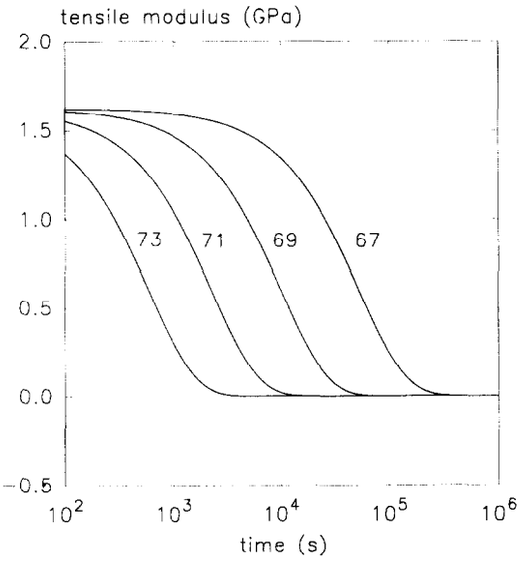

Figure 3 Simulations of tensile stress relaxation of non-equilibrium PET in the glassy state; the temperature was 50°C and different structural states were represented by the fictive temperatures (°C) shown. Otherwise, conditions were as for *Figure 1*. The model exhibits physical ageing

temperature dependence of G^b is neglected, all the results display close agreement with time–temperature superposition. From equation (18) the total shift factor $\ln(\tau_0/\tau_0^*)$ can be expressed as the sum of a time–structure shift factor and time–temperature shift factor:

$$\ln\left(\frac{\tau_0}{\tau_0^*}\right) = \ln a_e + \ln a_T \tag{27}$$

where

$$\ln a_e = C\left(\frac{1}{T_f - T_\infty} - \frac{1}{T_f^* - T_\infty}\right);$$

$$\ln a_T = \frac{\Delta H_0}{R}\left(\frac{1}{T} - \frac{1}{T^*}\right) \tag{28}$$

The model PET has a relaxation time τ_0 varying with temperature and fictive temperature as plotted in *Figure 4*. At high temperatures, in structural equilibrium ($T_f = T$), the relaxation time is a unique function of temperature, while at low temperatures where the structure falls out of equilibrium it depends on structural state (as expressed by T_f) as well as temperature. It is well known that amorphous polymers behave in this way near T_g, producing a kink in a plot of relaxation time *versus* temperature, and it is clearly visible in published data for PET[27]. Experimentally, however, it is difficult to obtain measurements under accurately isostructural conditions (constant T_f) near T_g, because of the problem of physical ageing occurring during the mechanical test; consequently, experimental data do not show the sharp transition between equilibrium and isostructural conditions apparent in *Figure 4*. With respect to the detailed temperature dependence of τ_0, it follows the Arrhenius equation under isostructural conditions below T_g (from the second of equations (28)) and approximates to the Vogel–Tammann–Fulcher equation above T_g (from the first of equations (28), which swamps the effect of $\ln a_T$ and is equivalent to

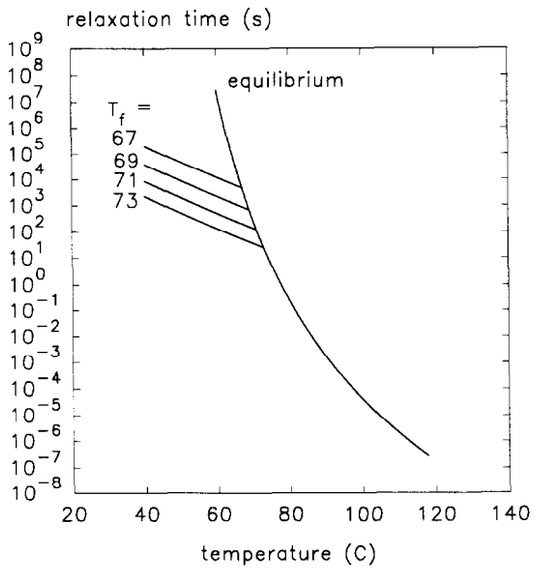

Figure 4 Linear viscoelastic relaxation time calculated for the PET model, showing the equilibrium curve and four representative branches for non-equilibrium structural states, corresponding to different values of fictive temperature (°C) shown

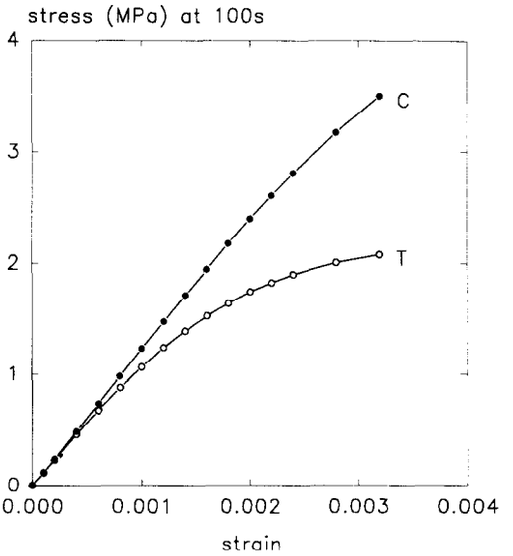

Figure 6 Stresses calculated in the same simulations as *Figure 5*, plotted isochronally for a time 100 s after strain was applied, *versus* strain level for tension (T) and compression (C). The model is clearly stiffer in compression than in tension

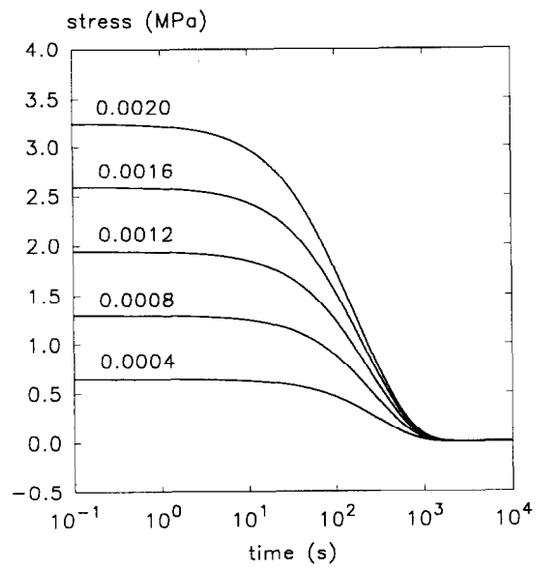

Figure 5 Simulations of uniaxial tensile stress relaxation of PET in the non-linear viscoelastic range, in equilibrium at 70°C. Strains shown were applied in 10^{-2} s ramps and then held constant. The time-scale of response shortens with increasing strain, as indicated, for example, by the inflection position

the WLF equation): the pattern shown by amorphous materials generally[21].

Non-linear viscoelasticity

To study the onset of viscoelastic non-linearity, simulations of uniaxial tensile stress relaxation were carried out at increasing values of axial tensile strain, again with the strain applied in a 10^{-2} s ramp and then held constant. Results are shown in *Figure 5*, for the model PET in equilibrium at a temperature of 70°C. Strain softening is clearly apparent: although the increments of strain are equal, calculated stresses are unequally spaced. The time-scale of response clearly shortens with increasing strain. From a series of such simulations, the 100 s isochronous stress was obtained and plotted in *Figure 6* (curve T). Similar simulations were carried out for stress relaxation in uniaxial compression, and 100 s isochronous stresses are also included in *Figure 6* (curve C). In addition to revealing the strain softening mentioned above, the results also reproduce another well-documented feature of the behaviour of amorphous polymers: the greater stiffness in compression than in tension[28]. Within the constitutive model it is a consequence of the pressure dependence of the activation barrier, through the influence of the pressure activation volume V_p.

A further non-linear feature that appears to occur generally in polymers is the pattern of response to load superposition: the response to the second load is stiffer, the longer the period for which the first load has been applied[29]. In the present model this is also observed. It follows from the fact that under constant stress or strain the deviatoric stresses are relaxing according to equation (23), and hence so is the octahedral shear stress τ_{oct}^{b}, and from equation (17) the viscosity μ is increasing with time. Several studies have been reported where this pattern of behaviour was observed by means of linear viscoelastic perturbation experiments, applied to a polymer specimen already loaded into the non-linear viscoelastic range. Particularly interesting are the results of Smith *et al.*[30], who superposed linear perturbations on polycarbonate stress relaxing under tension and compression. In both cases, the pattern of initial softening followed by time-dependent stiffening was observed, but with the modulus measured under compression being higher than that measured under tension[30]. The model exhibits similar behaviour. *Figure 7* shows the instantaneous relaxation time ratio $a = \tau/\tau_0$ at various times t during the same stress relaxation simulations as *Figure 6*. It can be seen that a decreases (indicating strain softening) upon loading, but then increases with time, and there is

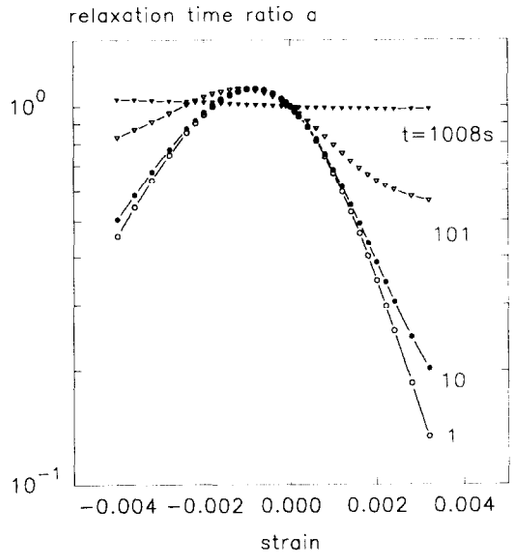

Figure 7 Instantaneous values relaxation time, expressed as the ratio $a = \tau/\tau_0$, calculated during the same simulations of non-linear stress relaxation as *Figure 5*, for various times t since application of strain. The primary effect is a progressive lengthening of the relaxation time during stress relaxation, giving the appearance of physical ageing (*Figure 3*), but in fact it is due to relaxation of the octahedral shear stress and mean stress, and their effects on the viscosity μ from equation (17)

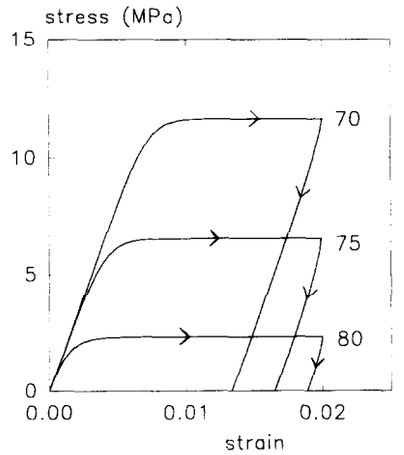

Figure 8 Simulations of a single tensile loading–unloading cycle through yield, on PET in equilibrium at the temperatures (°C) shown. Strain was ramped up and down at the rate $10^{-2}\,s^{-1}$, leaving an apparently permanent residual strain

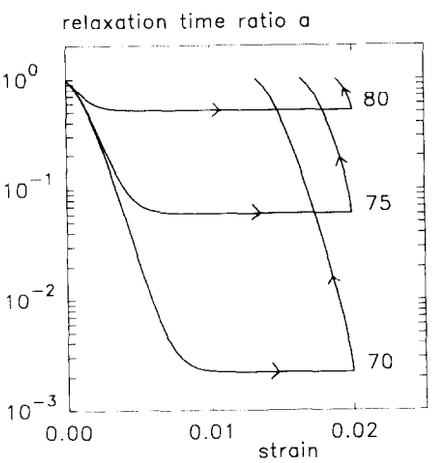

Figure 9 Instantaneous values of relaxation time, expressed as $a = \tau/\tau_0$, calculated during the same simulations as *Figure 8*, showing greatly varying degrees of deviation from viscoelastic linearity (deviation from $a = 1$)

asymmetry between tension and compression as observed experimentally. In terms of the model, asymmetry results from the effect of the mean stress, which is to increase τ in compression but to decrease it in tension.

Yield and pseudo-plastic flow

When amorphous polymers are strained further at the temperatures of interest here, they show an apparent yield, where stresses cease increasing and may indeed decrease. The deformation is then apparently 'plastic', appearing to be permanent when load is removed. As is well known, however, the deformation is recoverable if temperature is raised and hence 'pseudo-plastic' is a better description. The same pattern of response can be seen in simulations of drawing with the present model. Tensile loading–unloading cycles were simulated with a strain rate of $10^{-2}\,s^{-1}$ at various temperatures, producing stress–strain diagrams as shown in *Figure 8*. An apparent yield is clearly visible, with residual strain upon unloading. In terms of the model, 'yield' occurs when bond stretching ceases and the rate of flow due to self-diffusion of molecular segments matches the imposed rate of strain ($\dot{s}_i^b = 0$ in equation (23)).

When yield occurs at low temperatures, where the arguments of exponential and sinh terms in equation (17) are large compared with unity, we may recover other well-known features of the yield of polymers. Under these conditions, conformation stresses are negligible at typical yield strains, and τ_{oct}^b and $\Delta\sigma_m^b$ can be replaced by τ_{oct} and σ_m. Equation (13) may then be expressed in the form

$$\frac{V_s\tau_{oct}}{2RT} + \frac{V_p\sigma_m}{RT} = \ln d_{oct} + \ln\frac{\mu_0 V_s}{RT} \qquad (29)$$

at yield. This shows that for given rate of octahedral shear, temperature T and structure T_f, a pressure-modified von Mises yield criterion will be obeyed, as widely observed. Second, it shows that for given stress state, temperature and structure, stresses are linearly related to the logarithm of strain rate, again as usually observed (the well-known 'Eyring plot').

It is interesting to note, however, that the existence of an apparent yield does not depend upon viscoelastic non-linearity: it is a general feature of the Maxwell model-type of response represented by equation (23). Varying degrees of non-linearity at yield can be seen from the instantaneous values of relaxation time during the simulations of *Figure 8*, as shown in *Figure 9* as the relaxation time ratio a. It is clear that, under the conditions of the simulations, there is a high degree of non-linearity at 70°C, but it decreases with increasing temperature. As stress magnitudes fall, exponential and sinh terms in equation (17) eventually vanish compared with unity and the linear viscoelastic limit is reached. This is consistent with Retting's finding that amorphous polymers show a remarkably high degree of viscoelastic

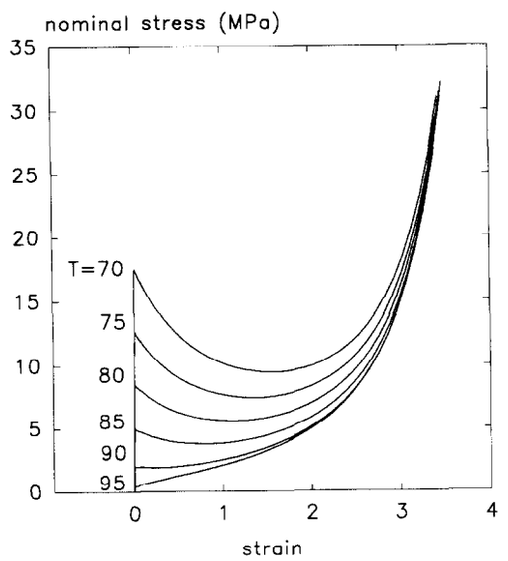

Figure 10 Simulations of uniaxial drawing of PET in equilibrium at the temperatures (°C) shown, expressed as nominal stress *versus* nominal strain, showing a (sharp) yield region followed by flow and strain stiffening

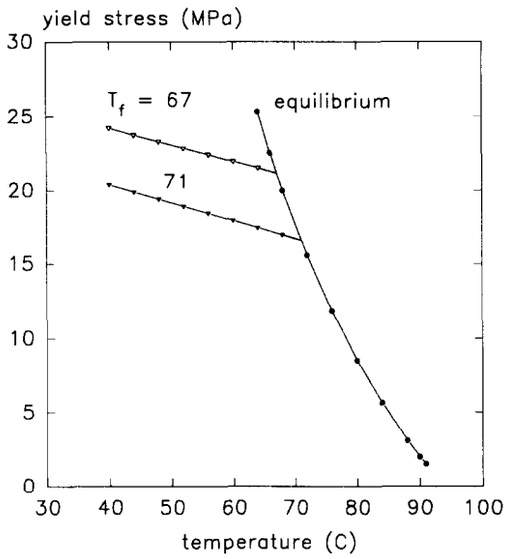

Figure 11 True 'yield stresses' calculated at the points of maximum nominal stress in simulations of uniaxial drawing at constant extension rate as in *Figure 10*, for PET in equilibrium (●) and in two non-equilibrium structural states (▽, ▼). The similarity to the behaviour of linear viscoelastic relaxation time (*Figure 4*) results from their common dependence on the limiting viscosity μ_0

linearity in tensile tests at temperatures 20 K or more above the glass transition[31], where maximum stresses are only of the order of 1 MPa.

Most experimental studies of hot-drawing (extension to large strains) have been conducted in uniaxial tension at a constant rate of extension. Tests of this form on PET were simulated with the model for a constant rate of extension of $1\ s^{-1}$. Some typical results are expressed as curves of nominal stress *versus* nominal strain in *Figure 10*. Two features are prominent and are characteristic of experimental data for amorphous polymers. One is the peak in nominal stress associated with ' yield', although the peak is much sharper than observed experimentally. In terms of the model, the peak is largely a geometric effect caused by the reducing cross-sectional area. Another, smaller contribution comes from the reduction in rate of natural strain in a test with constant rate of extension. The other prominent feature is the pronounced strain stiffening at large strains – a well-known feature of the drawing of polymers. In terms of the model, it arises from the non-quadratic form of the conformational free energy function given by equation (21), which in turn results from the non-Gaussian nature of the entropy function at large strains, because of chain straightening. The fact that such strain stiffening is associated with increasing alignment of molecular segments has been well attested to over many years by such techniques as optical birefringence, and n.m.r. and i.r. spectroscopies. In this region the simulated polymer is behaving as a molecular network, and it follows that it also exhibits the other network-like features revealed in studies of hot-drawing. In particular, Ward and co-workers have shown that drawing of partially pre-drawn PET produces a unique stress–strain curve when correct allowance is made for strain resulting from the previous draw[1,32,33]: excellent evidence for the existence of a molecular network.

The peak in nominal stress is frequently used operationally to define a yield 'point' in experimental data. In like manner, from stresses calculated during the simulation of drawing, a 'true yield stress' was determined as the true stress at the strain corresponding to the peak in nominal stress. Yield stresses obtained in this way are shown in *Figure 11* plotted *versus* temperature, for equilibrium PET ($T_f = T$) and for two non-equilibrium, isostructural cases (constant T_f). An upper temperature limit was provided by 91°C, as beyond this point the nominal stress–strain relation showed no peak in nominal stress at a strain rate of $1\ s^{-1}$ (see *Figure 10*). Two features are noteworthy in *Figure 11*. First, the form of the temperature dependence is as observed experimentally. Measurements of tensile yield stress reported by Allison and Ward for amorphous PET over a wide range of temperatures also showed a lower temperature coefficient below the glass transition than above[34]. In terms of the model, the origin of this is clear from equation (29). It simply reflects the temperature dependence of $\ln \mu_0$ which can be seen from *Figure 4*. The second feature follows from this. When the material is in a non-equilibrium glassy state below T_g, physical ageing represented here by a decrease in fictive temperature will cause a rise in yield stress due to the increase in μ_0. Such a rise in yield stress is widely observed during physical ageing of amorphous polymers, and was observed by Aref-Azar *et al.* in the specific case of PET[35].

DISCUSSION

It is clear that the constitutive model can account for many of the observed features of deformation of amorphous polymers near the glass transition. In particular, the features listed in the Introduction have all been replicated. Particularly satisfying is the fact that the model provides common explanations for effects that are normally treated as unrelated. One example has been highlighted already. Characteristic features of the temperature and structure dependences of both the linear

viscoelastic relaxation time and the yield stress arise from the same physical process, through the Newtonian limit of the viscosity, μ_0. Another example is the common origin of both the effect of pressure on yield, through the modified von Mises yield criterion, equation (29), and the different stiffnesses in tension and compression shown in *Figure 6*. Both arise from the effect of the pressure activation volume V_p, which reflects the assumption in the model that the flow activation event involves passage through a momentarily dilated state. A further example is the assumed additivity of stresses arising from perturbation of interatomic potentials on the one hand, and conformational entropy on the other. This is a fundamental feature of the model, necessary for the uniaxial stress response to show yield and flow typical of a glass at short times and low temperatures, and rubber elasticity at long times and high temperatures. In addition, however, it introduces other manifestations of parallel coupling, such as the time dependence of Poisson's ratio in uniaxial stress relaxation. Furthermore, it is consistent with the well-established analysis of stress in elastomers as the sum of an energy-elastic term associated with volume change and an entropy-elastic term associated with perturbation of molecular conformations.

The reader will note the model embodies another major assumption: there is only one mechanism whereby bond stretching stresses relax, operative throughout the range of strain. Thus the yield phenomenon is simply another perspective on the same flow process as that causing linear viscoelastic response at small strains. Previous authors have been reluctant to make such a far-reaching claim. In the work of Haward and Thackray[2], it was specifically excluded. Clearly, its validity should be tested by experiment. However, the present work has shown that a great many features of polymer behaviour can be explained within a simple constitutive framework on the basis of this assumption, and it therefore merits serious consideration.

In spite of its success, however, the form of constitutive model presented here has three major weaknesses. First, relaxation of the bond stretching component of stress is far too localized in the time domain. Stress relaxation in the glass transition region is confined to about one decade of time (see *Figures 1* and *3*), whereas it is well known in practice to extend over about five decades[20]. The present model reduces to a single relaxation time spring–dashpot-type of model in the linear limit, see equation (25), whereas it is necessary to generalize this to a spectrum of relaxation times to obtain a quantitative fit to measured stress relaxation data[20]. Similarly, yield as predicted by the model is confined to too small a range of strain. *Figure 8* shows yield occurring at strains of less than 10^{-2}, while measured yield strains are of the order of 10^{-1}. Babaiikochekseraii and Buckley[12] showed that generalization of the present model to the case where there is a distribution of energy barrier heights is equivalent to a generalized Maxwell model in the linear limit, and also produces the broadening of the yield region seen in experimental data.

A second unresolved issue is the question of structural evolution in amorphous polymers. In the model presented here, this would be represented by evolution of the fictive temperature T_f, following common practice in glasses[21]. As is well known, the structure of an amorphous polymer can evolve spontaneously below the glass transition (physical ageing), depending on the thermal history. How to describe analytically the kinetics of this evolution and hence predict the time dependence of T_f is, however, a matter of continuing debate, and has not been incorporated. It would clearly be a necessary feature of a more comprehensive constitutive model. A further unanswered question is the effect that stress history has on structural evolution. There is evidence that the drop in true stress at yield observed in polymers below the glass transition results from a process of de-ageing (increase in T_f), induced by the onset of plastic deformation[35]. The drop is greater for samples previously aged to lower values of T_f[35]. The work of Boyce *et al.*[5] includes a phenomenological description of plastic strain-induced structural evolution, and this can account for the drop in true stress at yield. In view of current uncertainty on the kinetics of structural change in glassy polymers, no attempt has been made to include them in the present model. All simulations with the model have been isostructural (T_f assumed constant), in which case there is no drop in true stress at yield if the rate of natural strain is constant. It has been argued sometimes that the observed time-dependent stiffening of glassy polymers under load, prior to yield, also results from structural change: stress-induced de-ageing followed by re-ageing. However, this interpretation has been challenged by other authors, and one of us has shown that the effect could also arise by a different mechanism: relaxation of microstress on a non-linear viscoelastic component of the microstructure[36]. This is illustrated in the present model by time-dependent lengthening of the relaxation time during isostructural stress relaxation (*Figure 7*), as the components of deviatoric bond stretching stress $\mathbf{S}^b$ relax.

A third outstanding issue is how to incorporate slippage of entanglements ('reptation'). At the highest temperatures and longest times, conformation stresses can relax by a process of axial diffusion of entire molecules, whereby they disengage from the topological constraint of other molecules. The effect is that the predicted bunching of stress–strain curves seen at high strains in *Figure 10* does not occur in practice in uncrosslinked polymers. With increasing temperature or time, strain stiffening is deferred to higher strains or may disappear completely, because of the contribution of entanglement slippage. More recent work in our laboratory has suggested means of incorporating this within the constitutive model[37], but details are beyond the scope of this paper.

Fourth, it should be recalled that the present paper has considered only non-rotational displacement fields. When the velocity gradient tensor contains a spin component, it must be partitioned between elastic and viscous displacements, in order to determine separately the elastic and viscous stretches. Boyce *et al.* addressed this issue, concluding that partitioning the spin differently had a negligible effect on predictions made with the constitutive model, and suggesting for convenience that spin be associated entirely with the viscous (in their work, plastic) displacement[38]. Further work is needed to verify this experimentally.

Finally, it is of interest to compare the present model with the constitutive model of Boyce, which has been applied with success to a wide range of measurements of

plastic deformation in glassy polymers. Both are glass–rubber models and in many respects behave similarly, but they are in fact structured differently. The present model assumes additivity of bond stretching and conformational stresses, equation (3), consistent with additivity of the corresponding terms in the free energy function, and existing physical theories are invoked for relations between these stresses and the strain state. The Boyce model contains an unphysical feature, however, in representing the actual material by a series-coupled combination of two separate materials: a linear elastic material (representing the unrelaxed glassy response) and an incompressible rubber constrained by a non-Newtonian viscous fluid, representing rubber-like response and flow of the glass. The two models show identical response in the linear viscoelastic limit of vanishingly small strains – they then correspond to equivalent forms of the Zener viscoelastic model. At large strains they differ, but it is difficult to quantify the differences as, to date, they have incorporated different descriptions of flow and rubber elasticity. The Boyce model invokes the Argon 'double-kink' model of flow[8], but this was not employed in the present work, as it is based on a localized flow activation event most appropriate to flow deep in the glassy region, whereas the present work is concerned primarily with the area of the glass transition. Boyce and co-workers have employed the 'inverse Langevin' expression for the end-to-end tension of a chain of random links, together with a three-chain (or latterly an eight-chain[39]) unit cell representation of the rubber, to represent the rubber elasticity in three dimensions. Another variant used in a Boyce-type model by Wu and Van der Giessen[16] is a linear combination of three-chain and eight-chain stresses. In the present work we have preferred to use the Edwards–Vilgis entropy function, in view of its more rigorous physical basis and greater convenience in use in our model. Further work is needed to compare the relative merits of these different approaches.

CONCLUSIONS

We have presented a three-dimensional glass–rubber constitutive model that exhibits most of the characteristic features of amorphous polymer behaviour near T_g. It takes the form of a coupled set of simultaneous non-linear differential equations, that may be solved numerically to simulate constitutive response of a polymer subject to a given history of stress or strain. The simulated material behaves as a glassy polymer at low temperatures and short times, and as a rubbery polymer at high temperatures and long times. There are three essential features. First, bond stretching stresses act in parallel with conformation entropic stresses, representing the additivity of corresponding terms in the free energy function. Second, bond stretching stresses relax by local self-diffusion of molecular segments. This is modelled conveniently by a three-dimensional adaptation of the generic activated rate process model of Eyring, enabling the model to exhibit the well-known features of yield and flow in amorphous polymers near T_g. Third, conformational entropy of the entangled molecules endows the model with the characteristics of a rubber–elastic network at large strains and high temperatures. Many forms of conformational entropy function have been suggested in the past, but here that proposed by Edwards and Vilgis has been used as it provides a good combination of sound physical basis and ease of use. The model behaves similarly to other glass–rubber constitutive models for describing yield and drawing in glassy polymers, notably those proposed by Haward and Thackray and, more recently, by Boyce and co-workers in their extensive work on the same theme. In the present work, however, we have gone further than before, and claimed that such a model encompasses a wider span of experimental conditions, temperatures, times and strain levels than has been suggested previously. A variety of simulations with the model have suggested this may be the case. If true, it has major theoretical and practical implications: it indicates a common physical origin for the processes of both small strain relaxation and yield and flow, and it suggests that constitutive modelling of polymers in an engineering context may be more straightforward than hitherto supposed. There is an urgent need for more extensive experimental testing, to determine the limits of validity of this claim.

ACKNOWLEDGEMENTS

The work was supported by ICI Films and the UK Science and Engineering Research Council under Grant GR/E57345. The authors are indebted to Dr D. P. Jones of ICI for advice and encouragement.

REFERENCES

1 Ward, I. M. *Polym. Eng. Sci.* 1984, **24**, 724
2 Haward, R. N. and Thackray, G. *Proc. Roy. Soc.* 1968, **A302**, 453
3 Halsey, G., White, H. J. and Eyring, H. *Text. Res. J.* 1945, **15**, 295
4 James, H. M. and Guth, E. *J. Chem. Phys.* 1943, **11**, 455
5 Boyce, M. C., Parks, D. M. and Argon, A. S. *Mech. Mater.* 1988, **7**, 15
6 Boyce, M. C. and Arruda, E. M. *Polym. Eng. Sci.* 1990, **30**, 1288
7 Boyce, M. C., Montagut, E. L. and Argon, A. S. *Polym. Eng. Sci.* 1992, **32**, 1073
8 Argon, A. S. *Phil. Mag.* 1973, **28**, 839
9 Boyce, M. C., Parks, D. M. and Argon, A. S. *Mech. Mater.* 1988, **7**, 35
10 Boyce, M. C., Parks, D. M. and Argon, A. S. *Int. J. Plasticity* 1989, **5**, 593
11 Arruda, E. M., Boyce, M. C. and Quintus-Bosz, H. *Int. J. Plasticity* 1993, **9**, 783
12 Babaiikochekseraii, S. and Buckley, C. P. '8th Int. Conf. on Deformation, Yield and Fracture of Polymers', Plastics and Rubber Institute, Cambridge, 1991
13 Amoedo, J. and Lee, D. *Polym. Eng. Sci.* 1992, **32**, 1055
14 Buckley, C. P., Jones, D. C. and Jones, D. P. '9th Annual Meeting of the Polymer Processing Society', Manchester, UK, 1993
15 Sweeney, J. and Ward, I. M. *Trans. I. Chem. E.* 1993, **71** Part A, 232
16 Wu, P. D. and Van der Giessen, E. *Int. J. Mech. Sci.* 1993, **35**, 935
17 Buckley, C. P., Jones, D. C. and Jones, D. P. *Polymer* submitted
18 Lee, E. H. *ASME J. Appl. Mech.* 1969, **36**, 1
19 Treloar, L. R. G. 'The Physics of Rubber Elasticity', 3rd Edn, Clarendon Press, Oxford, 1975
20 Ferry, J. D. 'Viscoelastic Properties of Polymers', 3rd Edn, John Wiley and Sons, New York, 1980
21 Scherer, G. W. *J. Non-cryst. Solids* 1990, **123**, 75
22 Cohen, M. and Turnbull, D. *J. Chem. Phys.* 1959, **31**, 1164
23 Macedo, P. B. and Litovitz, T. A. *J. Chem. Phys.* 1965, **42**, 245
24 Edwards, S. F. and Vilgis, Th. *Polymer* 1986, **27**, 483
25 Theocaris, P. S. and Hadjijoseph, Chr. *Kolloid-Z.u.Z.Polymere* 1965, **202**, 133

26 Struik, L. C. E. 'Physical Aging of Amorphous Polymers and Other Materials', Elsevier, Amsterdam, 1978
27 Vallat, M.-F., Plazek, D. J. and Bhusan, B. *J. Polym. Sci., Part B, Polym. Phys. Edn.* 1988, **26**, 555
28 Thomas, D. A. *Plastics and Polymers* 1969, **37**, 485
29 Turner, S. *Polym. Eng. Sci.* 1966, **6**, 306
30 Smith, T. L., Ricco, T., Levita, G. and Moonan, W. K. *Plastics and Rubber Processing and Applications* 1986, **6**, 81
31 Retting, W. *Colloid Polym. Sci.* 1979, **257**, 689
32 Long, S. D. and Ward, I. M. *J. Appl. Polym. Sci.* 1991, **42**, 1911
33 Gordon, D. H., Duckett, R. A. and Ward, I. M. *Polymer* 1994, **35**, 2554
34 Allison, S. W. and Ward, I. M. *Brit. J. Appl. Phys.* 1967, **18**, 1151
35 Aref-Azar, A., Biddlestone, F., Hay, J. N. and Haward, R. N. *Polymer* 1983, **24**, 1245
36 Buckley, C. P. *J. Phys. D: Appl. Phys.* 1977, **10**, 2135
37 Adams, A. M., Buckley, C. P. and Jones, D. P. 'Proceedings of the Polymer Processing Society European Regional Meeting', Strasbourg, France, 1994
38 Boyce, M. C., Weber, G. G. and Parks, D. M. *J. Mech. Phys. Solids* 1989, **37**, 647
39 Arruda, E. M. and Boyce, M. C. *J. Mech. Phys. Solids* 1993, **41**, 389